SYNGAS AND HDS CATALYSTS DERIVED FROM SULPHIDO BIMETALLIC CLUSTERS

M. DAVID CURTIS,* JAMES E. PENNER-HAHN, JOHANNES SCHWANK, OSWALDO BARALT, DANIEL J. McCABE, LEVI THOMPSON and GEOFFREY WALDO

Departments of Chemistry and Chemical Engineering, The University of Michigan, Ann Arbor, MI 48109-1055, U.S.A.

Abstract—The clusters, $Cp'_2Mo_2Fe_2S_2(CO)_8$ (MoFeS) and $Cp'_2Mo_2Co_2S_3(CO)_4$ (MoCoS) ($Cp' = \eta\text{-}C_5H_4Me$) have been supported on the refractory oxides, Al_2O_3, SiO_2, TiO_2, and MgO, and subjected to temperature programmed decomposition (TPDE) under flowing H_2. Typically, CO evolution commences near 100°C, followed by evolution of 1–2 Cp-ligands from 180 to 400°C along with small amounts of CO_2, CH_4, and H_2S or Me_2S. The resulting compositions are shown to be active catalysts for CO hydrogenation and hydrodesulphurization (HDS) of thiophene. Methane is the principal hydrocarbon product from CO hydrogenation except for MoFeS/MgO where high selectivity for C_2 products was observed. The activity and selectivity of MoCoS/Al_2O_3 for thiophene HDS closely resembles those of conventionally prepared "cobalt molybdate" catalysts. The cluster derived catalysts have been characterized by Mössbauer and X-ray absorption (XANES and EXAFS) spectroscopies. It is concluded that the clusters undergo oxidation by the surface upon loss of organic ligands.

Over the last decade, there has been growing interest in organometallic compounds supported on refractory oxides as catalysts for a variety of reactions, including partial oxidations,[1,2] olefin metathesis,[3] hydrogenolysis and hydrogenation,[4] carbonylation of nitro arenes,[5] hydroformylation,[6] and Fischer–Tropsch chemistry.[7–14] This interest is derived in part from the perception that catalysts with unusual selectivities may be produced from organometallic precursors, especially bimetallic clusters.

What are the advantages, if any, of using organometallic catalyst precursors? From the standpoint of thermodynamics, one may argue that for a given support (and here a dehydroxylated support is quite different from the hydroxylated form), for a given reactant composition and pressure, and for a given concentration of supported metal species, there is a macro-state of lowest chemical potential. One might expect (naively) no difference, then, in behaviour between catalysts prepared by starting with metals in a low oxidation state (organometallics) or by starting with metals in a high oxidation state (conventional preparation). The former will be

oxidized and the latter reduced under reaction conditions such that the final state will be the same for both catalysts.
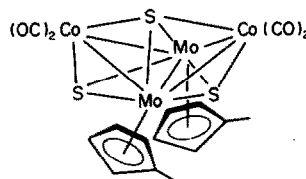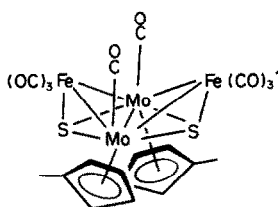
This analysis neglects the kinetics of the surface reactions and the mobility (or lack thereof) of the surface species. In actual practice, the surface species may be trapped in metastable states which differ depending on the initial conditions. Furthermore, the actual *compositions*, and hence final states, also depend on the initial conditions. For example, the decomposition of metal carbonyls may lead to the formation of metal carbides, whereas the counter ion (Cl^-, NO_3^-, SO_4^{2-}, etc.) of a high valent metal salt is also adsorbed on the surface during conventional preparative methods, and these counterions may affect the acidity of the support and the mobility of the metal species.

The answer to the question, "why use metal clusters?", is that one hopes to produce metastable states with desired selectivity which are not accessible from the conventional impregnation/reduction approach. The use of organometallic clusters as catalyst precursors has an additional advantage over conventional approaches, especially in the formation of bimetallic catalysts. Namely,

---

* Author to whom correspondence should be addressed.

the surface of bimetallic cluster-derived catalysts is much more uniform than those prepared by sequential- or co-impregnation methods because the two metals are deposited together in a well-defined spatial array and in relative amounts defined by the cluster composition. Spectroscopic studies of the active site are greatly facilitated when the surface is uniform.

This paper reports the preparation and characterization of catalysts derived from the bimetallic clusters, $Cp_2'Mo_2Fe_2S_2(CO)_8$ ("MoFeS") and $Cp_2'Mo_2Co_2S_3(CO)_4$ ("MoCoS"), $(Cp' = \eta\text{-}C_5H_4Me)$ whose structures are shown below.

CO_2, and CH_4 are also evolved at higher temperatures. Figures 1 and 2 are typical TPDE curves.

Table 1 lists the average surface composition, as determined from the TPDE results, after heating to 400°C. These compositions are obtained by subtracting from the initial composition the total moles of C and S evolved during TPDE. Since surface hydroxyl groups may contribute to the evolved hydrogen- and oxygen-containing species, it is impossible to quantify the remaining hydrogen or oxygen by this method.

The results in Table 1 show that in some cases, considerable CH_4 is evolved. This CH_4 may arise

EXPERIMENTAL
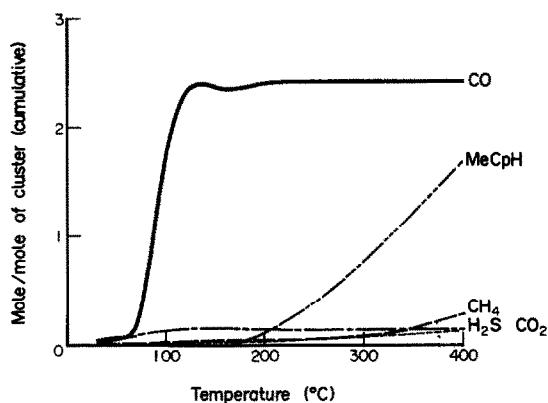
The clusters were synthesized as described previously,[15] and deposited on the oxide supports by contacting a CH_2Cl_2 solution of the cluster with sufficient support (previously calcined to 500°C) to give a 1 wt % total metal loading. Under these conditions, the cluster was completely absorbed and the solid was then collected by filtration and dried under vacuum at room temperature. On the Al_2O_3 (250 m² g⁻¹, a 1% loading corresponds to ca 8% monolayer coverage (ca 100 Å between clusters).

TPDE was conducted under flowing H_2 or He at 1 atm. pressure in an all glass system. Evolved hydrocarbons were analysed by GC/FID while CO, CO_2, and H_2S were measured by GC/TCD.

CO hydrogenations were performed in a glass-lined stainless steel differential flow reactor at CO : H_2 ratios of 3 : 1 to 1 : 1 and at pressures of 4–11 atm. Thiophene HDS reactions were performed in an all glass differential flow reactor with 2.8 mol % thiophene in H_2 (1 atm.) feed. Products were analysed as above and product identities checked by GC/MS.

RESULTS AND DISCUSSION

A. TPDE

Each combination of cluster plus support shows slightly different behaviour during TPDE. In all cases, a burst of CO is observed near 100°C, followed by gradual loss of Cp-ligand starting near 180°C. Small amounts of H_2S or Me_2S (never both),

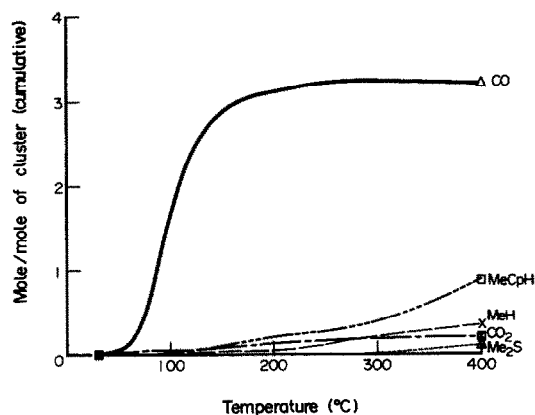Fig. 1. Temperature programmed decomposition (TPDE) profile of MoFeS/SiO₂ under flowing H₂.

Fig. 2. TPDE profile of MoFeS/MgO under flowing H₂.

Table 1. Number of retained carbon and sulphur atoms per adsorbed cluster following TPDE under H_2 to 400°C

Support	Al_2O_3	SiO_2	TiO_2	MgO
MoFeS	$C_5S_{1.8}$	$C_{5.5}S_{1.9}$	$C_8S_{1.5}$	$C_{10}S_{1.8}$
MoCoS	$C_{1.7}S_{1.8}$	$C_{5.9}S_{1.4}$	$C_{8.5}S_{1.5}$	$C_{7.8}S_{1.7}$

by cleavage of the methyl group of the Cp'-ligand or by reduction of CO groups with hydrogen derived from the surface hydroxyls. Only in the case of MoCoS/Al_2O_3 did the amount of evolved CH_4 correspond to the amount of evolved cyclopentadiene. In most other cases, the amount of evolved methane greatly exceeded the amount of evolved C_5H_6 so that most of the methane appears to come from CO reduction.

The total amount of carbon retained on the surface appears to increase as the basicity of the support increases. However, the utility and significance of these TPDE curves for determining surface composition is called into question by our EXAFS results (see below).

B. CO hydrogenation

The catalytic activity toward CO hydrogenation of these surface compositions has been determined. Table 2 lists the turnover frequencies (mol CO converted/mol supported cluster-s) and product selectivities for supported MoFeS (CO hydrogenation activity for MoCoS is currently under investigation). The numbers in parentheses are the corresponding values when 15 ppm H_2S is added to the feed stream.

The data in Table 2 show that methane is the principal product (except for MoFeS/MgO, see below) and that neither the TOF nor the selectivity is affected by 15 ppm H_2S. In contrast, H_2S acts as a severe poison for metallic catalysts. The selectivity for methane is highest for MoFeS/Al_2O_3. On SiO_2, about 20% C_2 (ethane + ethene) are produced along with small amounts of C_3 + hydrocarbons.

MoFeS/MgO shows an interesting transient behaviour (Figs 3 and 4). The catalyst starts by making methane almost exclusively. After a 24 h induction period, the activity for C_2 production rapidly increases, so that at $t = 25$–40 h, the product stream contains 90 mol % C_2 (ca 2:1 ethane:ethene). The C_2-activity gradually decays and reaches an apparent steady state which contains ca 75 wt % C_2 product. After 165 h on stream, the pressure was increased to 150 psig (1.11 MPa) which caused the methanation activity to increase relative to the C_2
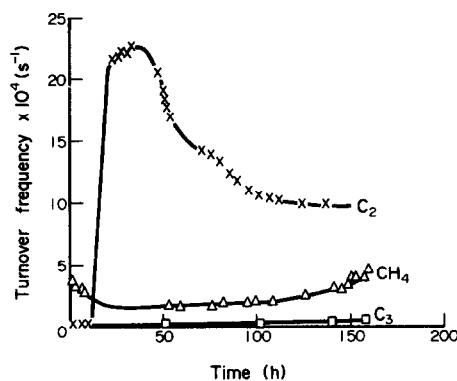

Fig. 3. Turnover frequency (mol product/mol cluster-s) for hydrogenation of CO over MoFeS/MgO at 400°C (3:1 H_2:CO, total $P = 0.37$ MPa).

Table 2. Turnover frequencies (mol CO/mol cluster-s) and product distributions for CO hydrogenation over MoFeS/Al_2O_3 at 400°C (3:1 H_2:CO)

Support	$P = 0.37$ MPa (40 psig)				$P = 1.11$ MPa (150 psig)			
	TOF^a	C_1	C_2	C_{3+}	TOF	C_1	C_2	C_{3+}
Al_2O_3	2.6	98	2	—	14	96	4	—
	$(2.5)^b$	(98)	(2)	—	(12)	(96)	(4)	—
SiO_2	9.3	77	18	5	49	81	17	2
	(9.0)	(17)	(17)	(6)	(47)	(80)	(16)	(4)
TiO_2	34	85	11	4	148	91	9	—
	(36)	(87)	(10)	(3)	(250)	(86)	(12)	(2)
MgO	60	28	68	4	90	56	34	10
	$(49)^c$	(84)	(12)	(4)	—	—	—	—

$^a \times 10^4$.
^{b} Numbers in parentheses are with 15 ppm H_2S in H_2.
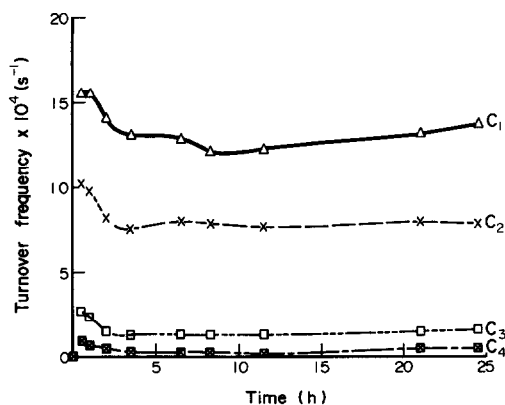^{c} Measured after high pressure run.

Fig. 4. Turnover frequency (mol product/mol cluster-s) for hydrogenation of CO over MoFeS/MgO at 400°C (3:1 H_2:C), total $P = 1.11$ MPa.

activity (Fig. 4). After 25 h at the higher pressure, the product stream contained 56 mol % methane, 34 mol % C_2, and 10 mol % C_{3+}. Decreasing the pressure to 40 psig (0.37 MPa) failed to restore the high C_2 selectivity; the product contained *ca* 85 mol % CH_4 and 10 mol % C_2 (i.e. had essentially the same composition as shown in parentheses in Table 2). This behaviour clearly demonstrates that a metastable state with high C_2 selectivity is initially produced, and that once the system is forced out of this metastable state, it cannot be regenerated from the final, stable state.

CO hydrogenation over MoFeS/Al_2O_3 also shows some interesting phenomena. An initial induction period (1–2 h) is observed, followed by a rapid rise in methanation activity. After about 10 h on stream, dimethyl ether begins to be produced. If the CO stream is interrupted, the system again repeats these induction periods when the CO stream is restored.

Figure 5 compares the product distribution obtained when the catalyst is pretreated under H_2 or He. The change in selectivity is reversible, i.e. the
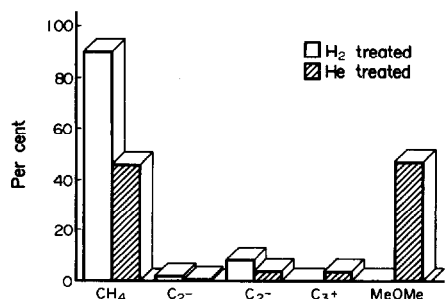

Fig. 5. Comparison of the product distribution for CO hydrogenation over MoFeS/Al_2O_3 as a function of catalyst pretreatment (3:1 H_2:CO, $T = 300$°C, $P = 0.37$ MPa).

product distribution depends only on the *immediate* pretreatment, not on the catalyst history.

At no time is H_2O or MeOH observed in the product. Therefore, we believe CO_2 and Me_2O are primary products, i.e. eqs (1) and (2) represent the reactions occurring.

$$2CO + 2H_2 \rightarrow CH_4 + CO_2 \tag{1}$$

$$3CO + 3H_2 \rightarrow Me_2O + CO_2. \tag{2}$$
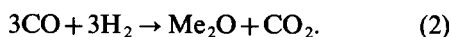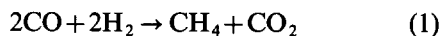
The kinetics of CO methanation over MoFeS/Al_2O_3 has been subjected to a Langmuir–Hinshelwood analysis.[16] It was shown that the rate of formation of methane follows the rate law given in eq. (3).

$$\text{rate} = k\frac{K_{H_2}K_{CO}P_{H_2}P_{CO}}{(1 + \sqrt{K_{H_2}P_{H_2}} + K_{CO}P_{CO})^2} \tag{3}$$

$$k = 3.22 \times 10^9 \exp(-135,000/RT)$$

$$K_{H_2} = 2.39 \times 10^{-8} \exp(54,100/RT)$$

$$K_{CO} = 7.00 \times 10^{-6} \exp(38,200/RT).$$

It can be shown[16] that this rate law is consistent with any Langmuir–Hinshelwood scheme in which the rate determining step contains one C-atom and two hydrogens. In particular, the CO insertion mechanism or the carbide mechanism,[17] with the rate determining step being either the hydrogenation of a surface formyl [eq. (4)] or the hydrogenation of a surface methylidyne [eq. (5)], respectively, with all other steps being in steady state gives rise to the observed rate law.

$$CHO(ads) + H(ads) \rightarrow CH_2O(ads) \tag{4}$$

$$CH(ads) + H(ads) \rightarrow CH_2(ads). \tag{5}$$
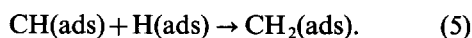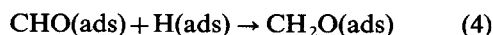
C. HDS activity

Table 3 shows the rates (mol thiophene converted/mol Mo-s) and product distribution observed for the hydrodesulphurization (HDS) of thiophene over MoCoS/Al_2O_3 at 300 °C (2.7 mol % thiophene in H_2 at 1 atm. pressure). Table 3 also compares these results with those obtained for a commercial catalyst (Catalco, *ca* 14% MoO_3/4% Co/Al_2O_3). Both catalysts were run in the non-sulphided form, i.e. after H_2 reduction at 400°C ("reduced" form) and after sulphidation with 10–15% H_2S in H_2 at 400°C. Reduced MoFeS/Al_2O_3 gave results very similar to those in Table 3. Trace amounts (< 1%) of butadiene were observed in all the catalysis runs.

Several things are apparent from the data in Table 3. First, the product distributions and activities of the MoCoS/Al_2O_3 and Catalco catalysts are nearly identical at the same level of conversion. This

Table 3. Turnover frequencies (mol thiophene converted/mol Mo-s) and product distribution for HDS of thiophene over $MoCoS/Al_2O_3$ and a commercial catalyst (2.7 mol % C_4H_4S in H_2 at 101 kPa, $T = 300°C$)

Catalyst	$TOF \times 10^4$	CH_4	C_2	C_3H_6	C_4H_{10}	1-C_4H_8	cis-2-C_4H_8	trans-2-C_4H_8	iso-C_4H_8
(A) Reduced									
$MoCoS/Al_2O_3$	1.5	3	13	37	1	6	10	12	18
Catalco	5.6	2	10	19	2	14	16	15	10
(B) Presulphided									
$MoCoS/Al_2O_3$	14	1	1	4	4	19	28	41	2
Catalco	14	1	2	6	3	22	27	37	3

strongly suggests that both catalysts have the same active site. Second, the cluster-derived catalyst shows a larger increase ($\times 10$) in activity upon presulphiding than the Catalco ($\times 2.5$). Third, the cracking activity (to propene, ethane, ethene, and methane) is much enhanced in the reduced form as compared to the sulphided form. Especially noteworthy is the relatively large amount of 2-methylpropene produced by the reduced catalysts. This product undoubtedly arises from isomerization of the butenes catalysed by acidic sites on the catalyst. Fourth, the ratios of the 1-butene: cis- and trans-2-butenes approach the equilibrium values (1 : 1.73 : 2.18), but there is always an excess of 1-butene. This suggests that 1-butene is the primary C_4-product and the 2-butenes are produced from isomerization of the 1-butene.

In control experiments, 1-butene in H_2 under identical conditions is isomerized to the mixture of butenes, but very little is hydrogenated and none is cracked. Butadiene, on the other hand, is hydrogenated to butenes and the amount of trans-2-butene is greatly in excess of its thermodynamic value. This suggests that the primary reduction product of butadiene is trans-2-butene. Again, no cracking of butadiene is observed. In another control experiment, tetrahydrothiophene was desulphurized under the same conditions over $MoCoS/Al_2O_3$. The products consisted of 99.6% butenes (55% 1-butene, ca 22% each of cis- and trans-2-butene) at 5% conversion.

One disturbing aspect of the product slate in Table 3 is the apparent lack of carbon balance. One would expect the amount of methane to equal the amount of propene, but this is not found (despite repeated calibration of the response factors). The balance of the carbon must be in an undetected product, e.g. MeSH, which is hidden under the large thiophene peak in the GC. Control experiments show indeed that MeSH has the same retention time as thiophene on our GC column. Mass spectral analysis of the thiophene peak is planned to detect the presence of MeSH.

D. *Mössbauer spectra*

The cluster, MoFeS, was prepared with enriched [57]Fe content and absorbed onto Al_2O_3. Table 4 presents the Mössbauer parameters obtained *in situ*. The pure, unsupported cluster shows an IS = -0.01 and QS = 0.80 mm s^{-1}. The supported cluster when oxidized in air shows only an Fe^{3+} signal with IS = 0.35 and QS = 0.98 mm s^{-1}

The supported clusters could be taken through repeated reduction–catalysis–oxidation cycles with the result that the same Mössbauer parameters as shown in Table 4 were re-established at each appropriate point in the cycle. This result indicates that the clusters are not sintering into larger particles in the course of these cycles.

The data in Table 4 clearly show that even under H_2, H_2/CO, or H_2/thiophene, the iron remains in an oxidized state (ca 90% Fe^{2+} and ca 10% $Fe^{\delta+}$). The species labelled $Fe^{\delta+}$ have Mössbauer parameters characteristic of Fe in highly covalent, organometallic complexes, although Fe^{3+} (tetrahedral) can also exhibit similar parameters.[18] However, the fact that this signal disappears immediately upon contact of the sample with oxygen, and reappears under H_2, suggests that the signal is due to a reduced species.

It is interesting to compare these data with those obtained on conventionally prepared catalysts. Vaishnava et al.[19] observed two signals with IS = 0.37, QS = 1.01 and IS = 0.35, QS = 0.73 mm s^{-1} in a sulphided $Fe/Mo/Al_2O_3$ sample. The first signal was attributed to a phase resembling iron aluminate in the alumina support, and the second to superparamagnetic particles of α-Fe_2O_3. Topsoe et al. observed signals with parameters, IS = 0.33, QS = 1.05 and IS = 1.06, QS = 1.78 in the Co emission Mössbauer spectrum of a sulphided $Co/Mo/Al_2O_3$ catalyst[20] which they attributed to the catalytically active Co—Mo—S phase. In view of our results and those of Vaishnava et al. it would appear that the latter signal is due to Fe^{2+} and the former to Fe^{3+}. In our system, the IS = 0.3, QS = 1.0 signal is

Table 4. *In situ* ^{57}Fe Mössbauer parameters for MeFeS/Al$_2$O$_3$ as a function of treatment

Conditions	Fe^{3+}			Fe^{2+}			Fe$^{\delta+}$		
	IS^a	QS^a	A%^{b}	IS	QS	A%	IS	QS	A%
25°C, air oxidized	0.35	0.98	100	—	—	—	—	—	—
400°C, H$_2$	—	—	—	1.07	1.86	90	0.07	0.31	10
320°C, H$_2$/CO (3:1)	—	—	—	1.08	2.06	87	0.17	0.61	13
25°C, air	0.34	0.98	95	1.06	1.95	5	—	—	—
400°C, H$_2$	—	—	—	1.07	1.89	100	—	—	—
320°C, H$_2$/CO (3:1)	—	—	—	1.09	2.07	93	0.09	0.44	7

^{a} IS = isomer shift, QS = quadrupole splitting, both ±0.05 mm s^{-1}.

^{b} A% = area per cent of fitted curves.

not observed during HDS catalysis, so the species responsible for this signal are probably not involved in the catalysis.

Another conclusion from the data in Table 4 is that the surface of the cluster-derived catalyst is remarkably uniform. There appears to be only one type of surface *ensemble* which is entirely oxidized to a single Fe^{3+} species, but which is reduced to an apparent equilibrium mixture of Fe^{2+} and Fe$^{\delta+}$. Alternatively, there are two sites (90% Fe^{2+} and 10% Fe$^{\delta+}$) which, upon oxidation, give rise to a single Fe^{3+} environment.

E. X-ray absorption spectra (XAS)

XAS were obtained on MoFeS/Al$_2$O$_3$ and MoFeS/MgO with (a) no heat treatment, (b) after heating to 120°C under H$_2$, and (c) after heating to 400°C under H$_2$. XAS of the pure, crystalline cluster were also obtained. Figures 6 and 7 show the near edge structure (XANES) of the Fe and Mo edges and Figs 8 and 9 are the Fourier transforms (phase
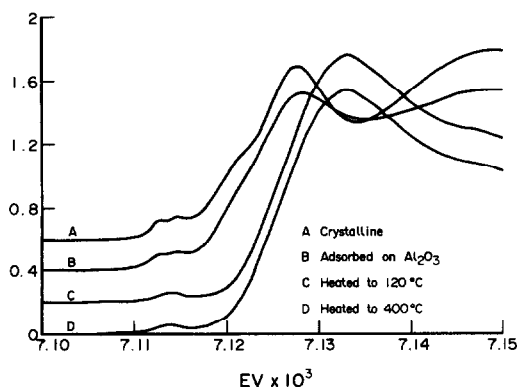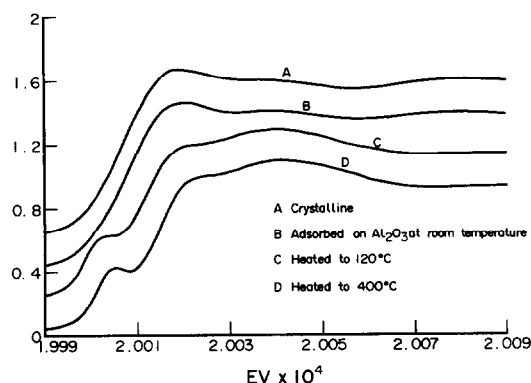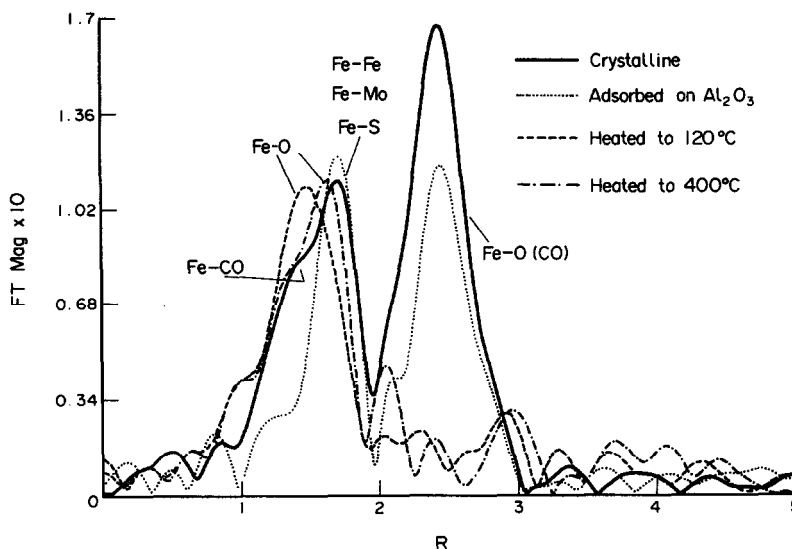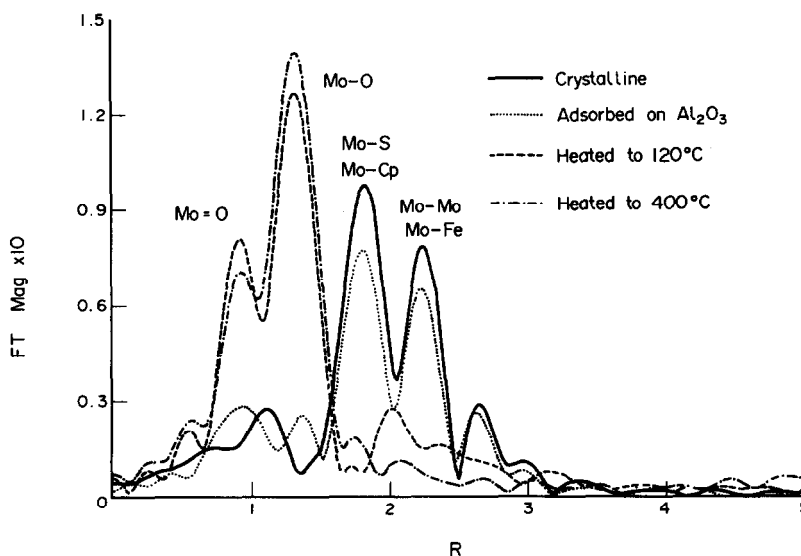

Fig. 7. Mo-XANES spectrum of MoFeS and MoFeS on Al$_2$O$_3$. Labels (A)–(D) are as in Fig. 6.

shifted radial distribution functions) of the Fe and Mo EXAFS, respectively, for MoFeS/Al$_2$O$_3$.

The Fe-XANES of the pure cluster and the cluster adsorbed on Al$_2$O$_3$ at room temperature (Fig. 6) are very similar. Both occur at essentially the same energy and both exhibit a pre-edge feature associated with a 1s–3d transition. The spectra of the two heated samples are identical and are shifted *ca* 5 eV to higher energies, an indication that the iron is now in a higher oxidation state. The pre-edge feature loses its structure, suggesting a more symmetrical arrangement of ligands about the iron.

Similar conclusions follow from the Mo-XANES (Fig. 7). The spectra of the pure cluster and the cluster on Al$_2$O$_3$ at 25°C are identical. Thus, the cluster is initially absorbed with essentially no change in the immediate environment of the Mo atoms. The spectra of the samples heated to 120 and 400°C under H$_2$ are nearly identical but different from the first two. The edges are shifted *ca* 5 eV to higher energies and a pre-edge feature appears which is attributed to the presence of one or more Mo=O bonds.

The phase-shifted radial distribution function (RDF) derived from the Fe-EXAFS (Fig. 8) shows

Fig. 6. Fe-XANES spectrum of MoFeS and MoFeS/Al$_2$O$_3$. (A) Pure crystalline cluster, (B) cluster on Al$_2$O$_3$ with no heat treatment, (C) on Al$_2$O$_3$ after heating to 120°C under H$_2$, (D) on Al$_2$O$_3$ after heating to 400°C under H$_2$.

Fig. 8. Fourier transforms of Fe-EXAFS of MoFeS and MoFeS/Al$_2$O$_3$.

Fig. 9. Fourier transforms of Mo-EXAFS of MoFeS and MoFeS/Al$_2$O$_3$.

two major peaks for the pure cluster. The first peak, with a shoulder at low R, corresponds to the unresolved Fe—S, Fe—Fe, and Fe—Mo distances (2.3–2.8 Å from the single crystal structure). Upon absorption on Al$_2$O$_3$, the peaks associated with the Fe—CO distances decrease in intensity. Curve fitting shows the adsorbed cluster has lost approximately 1.5–2 CO groups per Fe.

Upon heating to 120°C under H$_2$, all these peaks are lost and a new peak corresponding to Fe—O appears. Further heating the sample to 400°C causes a small change in the shape and position of this peak, but curve fitting shows both spectra can be fitted with six oxygen atoms at a distance of 1.95 Å from the Fe.

The environment around the Mo is revealed from the RDFs in Fig. 9. Both the pure crystalline cluster and the cluster adsorbed on Al$_2$O$_3$ show two peaks. The first is associated with Mo—S and Mo—C(Cp) (true distance ca 2.3 Å), and the second with Me—Fe and Mo—Mo vectors (true distance ca 2.8 Å). These peaks are replaced by Mo—O peaks when the sample is heated to 120 or 400°C under H$_2$.

Thus, the EXAFS and XANES spectra show that upon heating under H$_2$, both Fe and Mo are oxidized by the surface (most likely by the surface hydroxyl groups) to give oxide surface complexes. These results agree with the Mössbauer results which showed oxidation of the Fe to predominately

Fe²⁺ on the surface under actual working conditions. Furthermore, essentially all the oxidation/decomposition reactions are complete by 120°C. This picture contrasts with the TPDE results which show continuing evolution of hydrocarbon ligands from 180 to 400°C. It would appear that the cluster is oxidized at ⩽ 120°C and releases the hydrocarbon to the alumina surface. The TPDE experiment is then a measure of the activation energies required to release the hydrocarbon from the surface and is not a good indicator of cluster decomposition *per se*.

Preliminary EXAFS results obtained for MoFeS/MgO show much the same behaviour as for MoFeS/Al₂O₃. The major differences are that decomposition of the clusters already occurs at room temperature to give the surface oxo species and that long range order reappears in the EXAFS as the sample is heated under H₂ to 400°C. These data are currently under analysis, but preliminary results show the new long range order is not due to elemental iron or simple iron oxides.

F. Mechanistic conclusions

(a) CO *hydrogenation*. The combination of the product distribution, kinetics, and the Mössbauer and EXAFS characterization suggest that the active sites for CO hydrogenation activity of these clusters supported on metal oxides are surface oxo-ensembles. None of the data collected to date allows us to establish the structure of these surface ensembles, but it is clear that the "promoter", Fe or Co, plays an important role in defining the activity of these sites. On the basis of the data in hand, we propose the general mechanism shown in Scheme 1 for the production of CH_4, Me_2O, and CO_2 over these oxo-surface ensembles.

In this scheme, "M" represents the surface ensemble and may consist of more than a single metal atom. The *resting state* of the catalyst is proposed to be a metal oxo species, and is the most abundant species on the surface. This accounts for the fact that only minor changes in the Mössbauer parameters are seen *in situ* as the gas phase is changed from pure H_2 to H_2/CO.

The CO reacts with the oxo-ensemble to produce CO_2 (a primary product) with concomitant reduction in the oxidation state of the ensemble by two units [eg. $Mo(VI) \rightarrow Mo(IV)$ or $Mo(V) \rightarrow Mo(III)$]. Additional CO and H_2 then binds to the reduced ensemble. Insertion of the CO into an M—H bond leads to a surface formyl species which
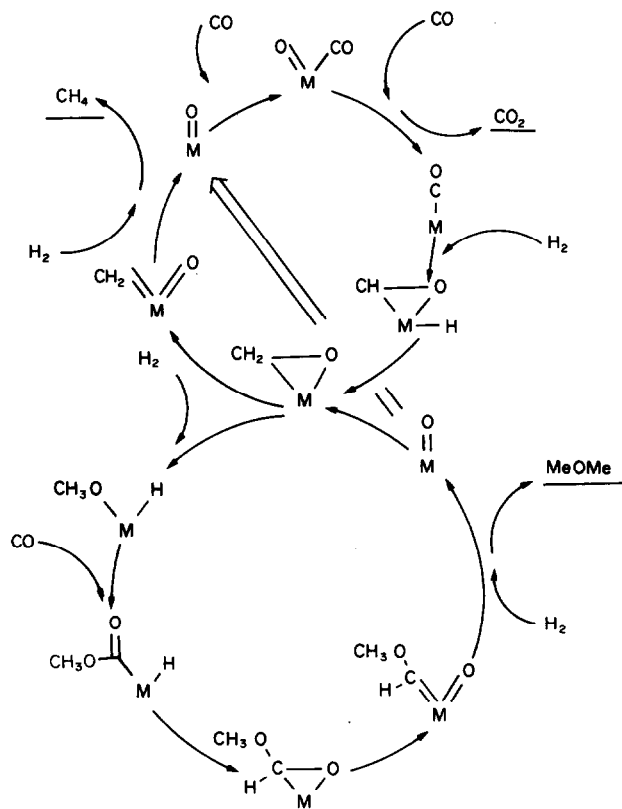
Scheme 1.

is hydrogenated to an adsorbed formaldehyde in the rate determining step. The surface formaldehyde may follow either of two reaction pathways: in path 1 (top circle, Scheme 1), this species is cleaved to a surface oxo-methylidene for which there are organometallic precedents.[21] The surface methylidenes may couple and lead to higher hydrocarbons, or be hydrogenated to methane to regenerate the resting state of the catalyst.

In path 2 (lower circle, Scheme 1), the surface formaldehyde is hydrogenated to bound methoxide. Absorbed CO then inserts into the M—OMe bond to produce a metalla-ester which is hydrogenated to a methoxyformyl. This formyl is then cleaved as in path 1 to an oxo-methoxymethylene which, upon hydrogenation, gives dimethyl ether (a primary product) and restores the resting state (M=O). Subtle changes in the surface induced by the pretreatment (H_2 or He) change the relative amounts of branching between the two pathways (cf. Fig. 5).

(b) *HDS of thiophene.* The Mössbauer parameters show that the catalyst surface changes very little when a stream of H_2 is replaced with a stream of H_2 +2.7% thiophene at 300°C. Under these conditions, the thiophene is desulphurized (checked by analysing the exit gases from the Mössbauer cell). The EXAFS shows that the predominant surface species under these conditions are metal oxo complexes. Therefore, MoS_2-like domains are *not* a necessary prerequisite for significant HDS activity of supported Mo HDS catalysts.

It is also interesting to note that neither the thiophene nor the small concentration ($\leqslant 0.05\%$) of H_2S produced in the differential flow reactor is capable of "sulphiding" the catalyst. Reactivity changes are noted when the catalysts are pre-sulphided with much higher concentrations (10–15%) of H_2S, however (see Table 3). We are currently collecting Mössbauer and EXAFS data on the supported clusters which have been pre-sulphided with H_2S in order to determine the effect of pre-sulphiding on the structure of the surface ensembles.

Some interesting conclusions may be drawn from the HDS product distribution when combined with the control experiments with 1-butene and butadiene. Since significant amounts of C_1, C_2, and C_3 hydrocarbons are produced during thiophene HDS, but none of these products is detected when 1-butene or butadiene is passed over the catalyst, it follows that the cracking must occur while the sulphur is still attached to the C_4 fragment. Furthermore, the fact that butadiene is rapidly hydrogenated to butenes, but the butenes are hydrogenated slowly, suggests an η^4-coordination for the

butadiene, which in turn implicates a π-bound thiophene in the HDS reaction.

Angelici and coworkers[22] have recently reported the synthesis of η^5-thiophene metal complexes and have presented model reactions of these complexes which implicate π-bound thiophene in the HDS catalysis. Furthermore, their data show that 2,3-dihydrothiophene is a likely intermediate in the HDS of thiophene.

Taken together, our data on the reactions of thiophene, tetrahydrothiophene, 1-butene, and 1,3-butadiene over $MoCoS/Al_2O_3$ suggest the mechanisms in Scheme 2.

The essentially complete conversion of tetrahydrothiophene (THT) to but*enes* at low conversion suggests that at least one of the desulphurization steps occurs by a "β-elimination" mechanism (Scheme (2a)). Butenes are also produced when THT is desorbed from an Mo(100) surface.[23] The fact that only traces ($< 1\%$) of methane, ethene, and propene are formed in the HDS of THT eliminates THT as an intermediate to these species in the HDS of thiophene. We therefore propose that thiophene is first hydrogenated to dihydrothiophenes which can then enter any of several reaction channels as shown in Scheme (2a). The adsorbed 2,5-dihydrothiophene (1) is the likely intermediate to butadiene.[22] Since so little butadiene is formed, the major route is apparently through the 2,3-isomer (2).

Adsorbed 2 is proposed to undergo C—C bond cleavage via 3 to eventually produce propene, methane, and methanethiol. Insertion into the C—S bond of 2 could give intermediate 4 which leads to butene as the major product through intermediate 5. An alternate minor path can lead to butenes or a metallacyclopentane 6. Intermediate 6 could scission by well documented pathways[24] to butene or to ethylene.

Clearly there is insufficient data to justify all the steps in Scheme 2. However, these were drawn so as to incorporate reasonable steps well known in organometallic chemistry which lead to the observed products. Current experiments are aimed at testing some of the proposed steps in Scheme 2.

SUMMARY

The results obtained to date show that sulphido bimetallic clusters are excellent precursors for the formation of uniform catalytic surfaces. The uniformity of the surface species facilitates physical characterization of the active site(s). Our results show that the supported clusters are transformed to surface oxo-ensembles which are active for

(a) HDS of tetrahydrothiophene

(b) HDS of thiophene
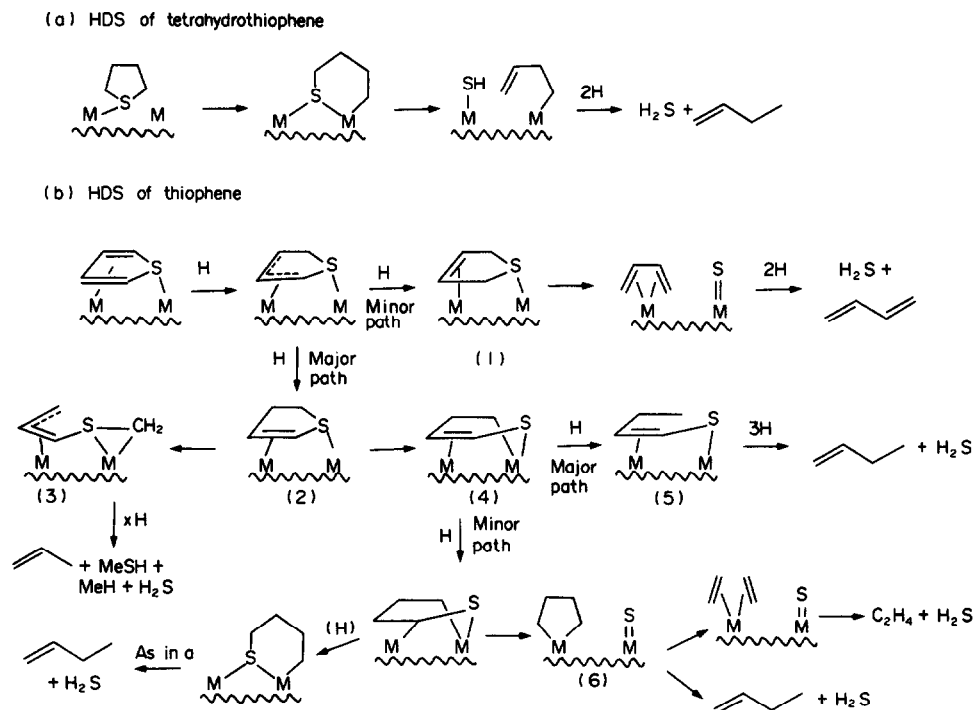
Scheme 2.

CO hydrogenation and HDS of organic sulphur compounds.

REFERENCES

1. (a) Y. Iwasawa and M. Yamagishi, *J. Catal.* 1983, **82**, 373; (b) Y. Iwasawa, Y. Sato and H. Kuroda, *ibid.* 289.
2. O. Leal, M. R. Goldwasser, H. Martinez, M. Garmendia, R. Lopez and H. Arzoumanian, *J. Molec. Catal.* 1983, **22**, 117.
3. (a) A. F. Danilyuk, V. L. Kuznetsof and Y. I. Ermakov, *Kinet. Katal.* 1983, **24**, 926; (b) A. Brenner and R. L. Burwell Jr., *J. Catal.* 1978, **52**, 364.
4. R. Nakamura, R. G. Bowman and R. L. Burwell Jr., *J. Am. Chem. Soc.* 1981, **103**, 673.
5. P. Braunstein, R. Bender and J. Kervenal, *Organometallics* 1982, **1**, 1236.
6. M. Ichikawa, *J. Catal.* 1979, **59**, 67.
7. J. Zwart and R. Snel, *J. Molec. Catal.* 1985, **30**, 305.
8. Yu I. Yermakov, *J. Molec. Catal.* 1983, **21**, 35.
9. J. M. Basset and A. Choplin, *J. Molec. Catal.* 1983, **21**, 95.
10. R. Ugo and R. Psaro, *J. Molec. Catal.* 1983, **20**, 53.
11. D. C. Bailey and S. H. Langer, *Chem. Rev.* 1981, **81**, 109.
12. E. L. Meutterties and M. J. Krause, *Angew. Chem., Int. Ed. Engl.* 1983, **95**, 135.
13. Y. Iwasawa (Ed.), *Tailored Metal Catalysts.* D. Reidel, Boston, MA (1986).
14. Yu I. Yermakov, B. N. Kuznetsov and V. A. Zakharov, *Catalysis by Supported Complexes.* Elsevier, Amsterdam (1981).
15. (a) P. D. Williams, M. D. Curtis, D. N. Duffy and W. M. Butler, *Organometallics* 1983, **2**, 165; (b) M. D. Curtis and P. D. Williams, *Inorg. Chem.* 1983, **22**, 2661.
16. L. T. Thompson Jr., J. Schwank and M. D. Curtis, submitted to *J. Catal.* (1988).
17. C. Masters, *Adv. Organomet. Chem.* 1979, **17**, 61.
18. C. Wivel, B. S. Clausen, R. Candia, S. Morup and H. Topsoe, *J. Catal.* 1984, **87**, 497.
19. P. P. Vaishnava, P. A. Montano, R. E. Tischer and S. S. Pollack, *J. Catal.* 1982, **78**, 454.
20. H. Topsoe, B. S. Clausen, R. Candia, C. Wivel and S. Morup, *J. Catal.* 1981, **68**, 433.
21. J. H. Wengrovius and R. R. Schrock, *Organomtallics* 1982, **1**, 148.
22. (a) A. Lesch, J. W. Richardson Jr., R. A. Jacobson and R. J. Angelici, *J. Am. Chem. Soc.* 1984, **106**, 2901; (b) G. H. Spies and R. J. Angelici, *ibid.* 1985, **107**, 5569.
23. J. T. Roberts and C. M. Friend, *J. Am. Chem. Soc.* 1986, **108**, 7204.
24. (a) J. D. Fellmann, G. A. Rupprecht and R. R. Schrock, *J. Am. Chem. Soc.* 1979, **101**, 5099; (b) J. X. McDermott and G. M. Whitesides, *ibid.* 1976, **98**, 6521; (c) R. H. Grubbs, A. Miyashita, M. Liu and P. Burk, *ibid.* 1978, **100**, 2418.